BROADBAND MULTI-MODE OUTPUT FROM MODULATED TWO-SECTION SEMICONDUCTOR LASERS

R Coyle[1], D M Kane[1], P Rees[2], I Pierce[2], D Masanotti[3], F Causa[3], T Ryan[3], and J Sarma[3]

[1]Department of Physics, Macquarie University~Sydney, NSW 2109, Australia
e-mail: debkane@physics.mq.edu.au

[2]School of Informatics, University of Wales, Bangor, UK

[3]Department of Electrical and Electronic Engineering, University of Bath, Bath, UK

ABSTRACT

A broadband multi-mode output with optical frequency bandwidth of several THz has been obtained by a method of modulating a two-section semiconductor laser (TSL). The comb-of-modes output can be systematically varied in bandwidth and opens up a new range of applications for TSLs.

1. INTRODUCTION

A method of operation of a two section semiconductor laser that allows a controllable, broad bandwidth output, (up to several terahertz, made up of many tens of longitudinal modes) by modulating the injection current to the shorter of the two sections, has been developed [1]. Both sections have forward dc bias currents, with the longer, laser section biased above threshold while the "absorber" section has a small (or indeed no) forward bias to which the ac modulation current is added. The bandwidth can be varied controllably by changing the depth of modulation, the absorber dc current and/or the frequency of the modulation. This type of operation has not been reported previously, to our knowledge, and represents a significant new method of producing broad bandwidth output from semiconductor lasers. Such controllable, broad bandwidth output has applicability in imaging where the variable optical bandwidth can be translated to variable resolution, spectroscopy and sensing, optical metrology and optical communications. These applications for TSLs are additional to those already identified: photonic switching, optical gates, optical clock synchronization and FSK (frequency shift keyed) transmitters.

The mechanism by which the bandwidth broadening is achieved has been elucidated by modifying the Yamada model describing any laser which has two spatially differentiable regions experiencing different gain and loss, such as a two-section laser or a quantum dot laser (QDL), to include a modulated current to the absorber section. In this case it is seen that loss modulation of the absorber section at frequencies which are a significant fraction of the relaxation oscillation frequency through to frequencies well above the relaxation frequency can not be "smoothed-out" through relaxation processes because of the rapid time scale of the modulation compared to the relaxation period. Thus, the effectiveness of the normal mode competition mechanisms is reduced. By changing the frequency (close to the relaxation oscillation frequency) or depth of the modulation the number of modes "released" from mode competition, and which then oscillate, is increased. Reverse biasing the absorber section has been predicted to enhance this effect even further by introducing larger differentials in the carrier lifetimes in the two sections (laser and absorber) for the case of quantum dot lasers.

2. EXPERIMENT

The experimental set-up is shown schematically in Figure 1. The TSL was a quantum well device ($In_{0.17}(Al_{0.125}Ga_{0.875})As_{0.83}$) lasing at ~850 nm. It was a cleaved-cleaved device with a laser section 375 μm in length and an absorber section 125 μm in length, fabricated at the University of Bath. The output was single transverse mode. With no modulation applied the laser output was multi-mode, with ~4-5 longitudinal modes in the optical frequency spectrum, typically. The TSL was mounted on a heat sink and temperature controlled. Light from the laser was collimated using a 0.23 pitch GRIN rod lens (Melles Griot # 06LGT214).

The optical frequency spectrum was observed using a scanning Fabry-Perot interferometer (FP) set-up with a free spectral range (FSR) of 2.2 THz (Burleigh RC-43), photodiode detection and an oscilloscope. An optical isolator was used to prevent unwanted feedback from the Fabry-Perot interferometer re-entering the semiconductor laser. This optical frequency spectrum measured was time-averaged over about one hundred nanoseconds. Forward dc injection currents I_L and I_A were applied independently to the laser and absorber

0-7803-7571-8/02/$17.00 ©2002 IEEE

sections of the device, respectively. A sinusoidal modulation current I_M, at frequency f_M, was added to the forward bias injection current to the absorber section using a signal generator (Rhode and Schwarz SMP22) and a bias tee. The modulation power P_M set on the signal generator was the quantitative measure, related to I_M, made in the experiment. The electrical connections to the device were simple ohmic contacts of wires so there was a variable coupling of the modulation power, as a function of frequency, to the absorber section, which was not controlled nor optimized in the experiments. Characterisation of the direct modulation transfer for the as-mounted device, operated as a single section laser by electrical connection of the two sections, shows a rapid roll-off in modulation above 950 MHz. It also shows that the device (as connected) has a larger modulation transfer for low frequency modulation (<200 MHz in particular).

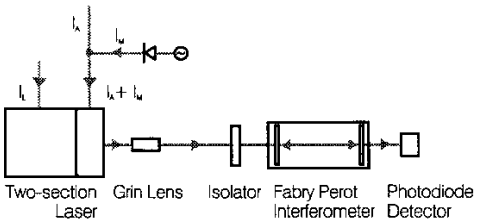

Fig.1: A schematic of the two-section laser showing injection currents to the two-sections and the diagnostics for monitoring the optical frequency spectrum.

Output power was monitored with an Ophir power meter. The output power versus laser-section injection-current was of standard form for absorber-section bias current of 1.5 mA or greater. The threshold current dropped as I_A increased, being 18 mA when I_A was 1.5 mA, reduced to 12 mA at I_A = 5mA. When the absorber current was less than 1.5 mA the output power versus laser-section injection-current showed a switch-on step in output power at a higher threshold current (21.5 mA at I_A = 1.0 mA and 23 mA at I_A = 0.5 mA) but thereafter has a similar slope efficiency as for higher values of I_A. The slope efficiency was 0.33 mW/mA, above I_{th}. The output power versus time using fast photodiode detection (risetime < 30 ps), and the RF noise spectrum of this signal were also monitored to identify any pulsing, mode-hopping, mode-locking or unstable behaviours. No measurable differences in these quantities have so far been observed for the different combinations of I_A, I_L, I_M and modulation power that have been investigated to date. This does not rule out such variations for individual modes but indicates they do not appear for the sum of all the modes. It remains for further study to test for such variations in spectrally-filtered, individual modes.

3. EXPERIMENTAL RESULTS

The results of having a fixed value for each of I_L(64.9 mA, ~4I_{th}), I_A (2.0 mA), and modulation frequency (960 MHz), and varying the modulation power (and hence I_M) is shown in fig.2. This modulation frequency is close to the relaxation oscillation frequency for the heavily damped TSL. It is seen that the optical frequency spectrum is similar to that for the free running TSL (fig. 2(a)) when the modulation power is low and then broadens in a controllable manner as the modulation power is increased. It is of the order of the 2.2 THz free spectral range (FSR) of the Fabry Perot interferometer in fig. 2(d). As the modulation power is further increased to 20 dBm the bandwidth broadens further to be of the order of 4 THz. This is seen by a doubling in the number of mode peaks within one FSR as the modes in the adjacent interference orders of the Fabry Perot become interleaved with those within a single order, as the spectrum broadens beyond the FSR.

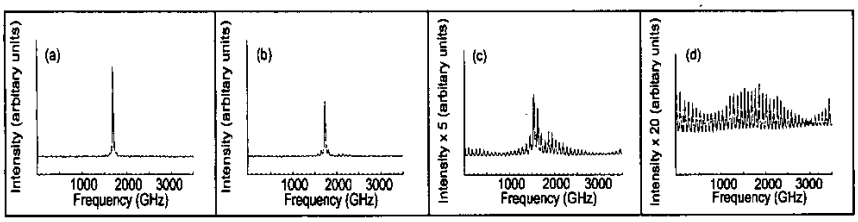

Fig. 2. The optical frequency spectrum from the TSL with I_L = 64.9 mA, I_A = 2.0 mA, f_M = 960 MHz and variable modulation power: (a) 0 bBm, (b) 2 dBm, (c) 7.6 dBm and (d) 15 dBm. The frequency scale is relative and centred about the laser wavelength of ~850 nm.

The bandwidth of the optical frequency spectrum as a function of modulation frequency, for fixed modulation depth and dc injection current to the laser section and absorber section, is shown in fig. 3. The optical bandwidth follows a form similar to the direct modulation transfer function. At all modulation frequencies, the optical frequency bandwidth can be further increased by increasing the modulation depth and/or decreasing I_A. The optical frequency bandwidths far exceed those achievable by direct modulation of the injection current to the laser section of the device.

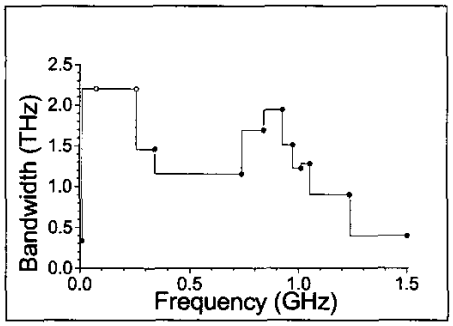

Fig. 3: Bandwidth of the optical frequency spectrum as a function of modulation frequency for I_L = 69.5 mA, I_A = 2.0 mA and modulation power = 7 dBm. Closed circles correspond to a bandwidth below the FSR of the FP interferometer, open circles indicate the bandwidth exceeded that of the FSR.

4. THEORY

The model to describe the two-section laser (and also quantum dot lasers) has been based on Yamada's model [2] developed to predict self pulsations in narrow stripe lasers. The self pulsation arises because of the differential gain and absorption in the central stripe relative to the absorbing regions immediately parallel of this stripe, on either side. The rate equations for the carrier density in the laser section, n_L, carrier density in the absorber section, n_A, and the cavity photon density, S_l are given in equations 1-3, respectively.

$$\frac{dn_L}{dt} = \frac{J_L}{wq} - \frac{J_{spon\_L}}{wq} - \sum_l g(\omega_l) S_l v_g \qquad (1)$$

$$\frac{dn_A}{dt} = \frac{J_A}{wq} - \frac{J_{spon\_A}}{wq} + \sum_l a(\omega_l) S_l v_g \qquad (2)$$

$$\frac{dS_l}{dt} = \left(g(\omega_l) - a(\omega_l) - \alpha\right)\Gamma S_l v_g + \beta\left(\frac{J_{spon\_L}}{wq} + \frac{J_{spon\_A}}{wq}\right) \qquad (3)$$

J_L is the current density to the laser section. J_A is the current density to the absorber section and when modulation is applied this takes the form:

$$J_A = J_{A0} + J_M \sin(2\pi f_M t)\,. \qquad (4)$$

J_{spont_L} and J_{spont_A} are the current densities arising from spontaneous emission in the laser and absorber sections, respectively. The carrier charge is q, w is the active layer thickness and v_g is the modal group velocity. $g(\omega_l)$ is the gain and $a(\omega_l)$ is the absorption (negative gain), as a function of angular frequency ω_l, in the laser section and absorber section, respectively. These were calculated using a many body quantum well (QW) gain calculation described in [3] and references there-in, for the QW TSL. For QDLs the gain, absorption and effective spontaneous emission current were calculated for an active layer composed of an ensemble of lens-shaped, self assembled, quantum dots. The effects of the inhomogeneous broadening of the gain spectrum that arises due to the variation in the sizes of the dots was also included. Calculating these also requires a value of the confinement factor, Γ, for the quantum well or quantum dots. The optical loss factor is α and β is the spontaneous emission coupling factor.

5. THEORETICAL SIMULATIONS

5.1 QUANTUM WELL TSL

In the simulations that have been carried out to date for a QW TSL, modest broadening of the optical frequency spectrum has been simulated for absorber-section reverse-biased-modulation. Significant broadening for forward bias of the absorber section is not observed in the simulations. This indicates that the devices used in the experiments are not well described by a QW gain and, are more likely to have characteristics like "bulk" semiconductor laser devices. For the results presented in fig. 4 a pulsating dc modulation on the absorber was used. J_{A0} was zero and J_A was $J_M \sin(2\pi ft)$ for the positive half-cycles and zero for the negative.

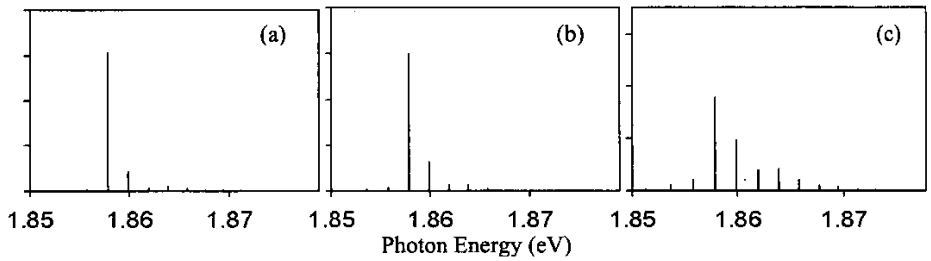

Fig. 4: Optical frequency spectra (time averaged for 10 ns) from QW TSL simulations with J_L=1500A/cm^2, f_M=3.5GHz, v_g=0.75x10^{10} cm/s, Γ=0.05, β=(10^{-5}/23) and J_M: (a) 0, (b) 400 A/cm^2 and (c) 800 A/cm^2. Device length: laser section 240 μm; absorber section 60μm.

5.2 QUANTUM DOT LASER

In contrast to the simulations so far completed for the QW TSL, simulations of QD lasers have generated optical frequency spectra with significant broadening for the case of a forward biased absorber section, as shown in fig. 5. The modulation frequency is increased, all other parameters being kept constant for the optical frequency spectra in fig.5. In this case a broadened gain bandwidth is realized because of the distribution of sizes of the quantum dots. This bandwidth can be accessed by modulating the absorber section.

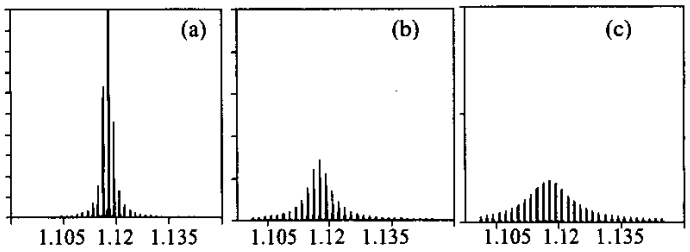

Fig. 5: Optical frequency spectra for QDL simulations with v_g=7.5x10^9 cm/s, Γ=0.03, β=1x10^{-5}, constant J_L, J_{A0}, and J_M; and f_M: (a) 100MHz, (b) 500 MHz, (c) 1 GHz. Device length: laser section 85 μm; absorber section 15μm. The power is in arbitrary units. The tick marks are spaced by 20.

6. DISCUSSION AND CONCLUSION

Optical frequency bandwidths in excess of 4 THz have been generated by modulating two-section lasers. Simulations of QDLs give similar broadening due to rapid loss modulation that can not be averaged out by relaxation oscillations. Simulations of QW TSLs have yet to identify laser parameters that generate the broad bandwidth observed experimentally, probably indicating a non QW-type gain for the actual devices.

REFERENCES

1. R Coyle, D M Kane, J Sarma, D Masanotti, T Ryan and P Rees, Proceedings of the Australasian Conference on Optics, Lasers and Spectroscopy, ACOLS 2001, Paper M22, pg 108. ACOLS 2001, Brisbane, Australia.
2. M Yamada, IEEE J Quant. Electron. **29**, 1330-1336, 1993.
3. I Pierce et al., Phys. Rev. A, **61**, art. No. 053801, 2000.